CHAPTER 1

Introduction and Scope of the Thesis

Contents

CHAPTER 1

Introduction and Scope of the Thesis

1.1 Solar Cell

Modernization and urbanization of societies and industries have significantly increased the use of energy in everyday life. Over the past several years, increased consumption of non-renewable resources like coal, petroleum, and gases will exhaust all the available natural sources [1]. The limited resources of fossil fuels and environmental pollution caused by the burning of fossil fuels have primarily encouraged the researchers for clean and green energy harvesting through renewable energy sources to meet the high demand for energy in the various electrical and electronic applications [2]. The major non-renewable and renewable sources are shown in Figure 1.1.

Solar energy is considered one of the most important renewable sources to solve the present and future energy problems because of its abundant availability and pollution-free generation [3]. Solar energy is converted to electrical energy by a typical solar cell, which has the edge of resolving large energy demand, less effect on climate change, control global warming, clean and unlimited energy source [3]. Various types of solar cells are fabricated using different photoactive materials, namely silicon, germanium, gallium arsenide, cadmium telluride, dyes, conducting polymers, perovskites, etc. [4]. The power conversion efficiency (PCE) of the solar cell primarily depends on photoactive materials and the device

structures.

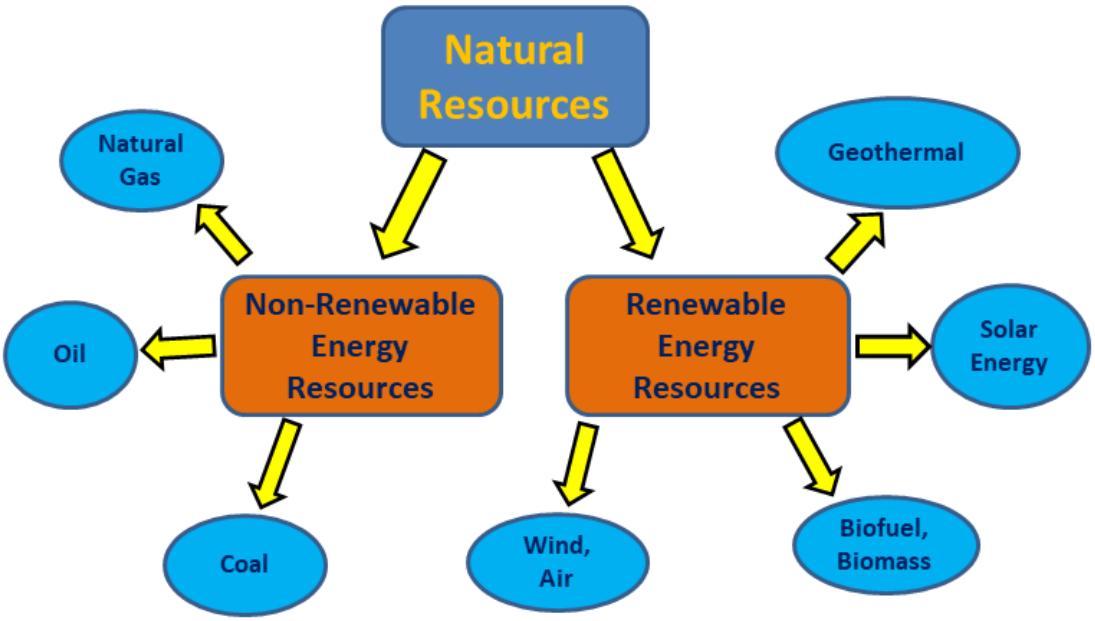

Figure 1.1: Various non-renewable and renewable energy sources.

1.1.1 Origin of Solar Cells

The Concept of the photovoltaic effect was first experimentally discovered by French physicist Edmond Becquerel in 1839 [5]. Later, Willoughby Smith passed an electric current through selenium and found the effect of light on electric current in 1873 [6]. He described that the light is striking a photosensitive semiconductor material result in electrical energy. This remarkable discovery is considered as the beginning of the new era for the conversion of solar energy into electrical energy using a solar cell [7]. In 1883, Charles Fritts invented the first solid-state photovoltaic (solar) cell using the thin film coating of gold on light-sensitive material selenium to form the junctions [8]. Although this device had only 1% efficient, it paved the way for future solid-state photovoltaic devices [8]. In 1905, Albert Einstein proposed a new theory of quantum physics and described the photoelectric effect [9]. The research on photovoltaic cells

was revolutionized after experimental validation of Einstein's photoelectric theory in 1916 and the Nobel Prize to Albert Einstein in 1921 [9].

Further, p-n junction based solar cells using Cu_2O and Ag_2S was reported by Vadim Lashkaryoy in 1941. The modern device structure of the junction based solar cells was proposed by Russell Ohl [10] in a patent filed in 1946. The first commercial standard solar cell having 6% power conversion efficiency (PCE) was developed using inorganic materials by Daryl Chapin, Calvin Fuller, and Gerald Pearson in Bell Laboratory in 1954 [11]. Later, the production of solar cells was started for commercial use. The first silicon-based solar cell panel was incorporated into US satellite Vanguard 1 in 1958 [Internet Source]. Several satellites such as Explorer III, Vanguard II, and Sputnik-3 were launched with solar cell-powered system onboard in the next few years.

1.1.2 Generation of Solar Cells

Silicon (Si) is the most widely used material in the electronic industry for the last seven decades. Fabrication of Si-based solar cells requires high-temperature processing and various sophisticated requirements, including nanofabrication facilities, ultra-high vacuum deposition process, etc. Further, the preparation of Si from silica is a high energy draining method, which makes very low energy payback time (EPBT) of the silicon-based solar cells. Moreover, the management of extremely large e-wastes resulting from the worldwide use of solar cells made of Si and other inorganic semiconductors have become a challenge for environment and water management systems. Thus, rigorous research is focusing on developing organic and hybrid semiconductors for environment-friendly and low-cost solar cells. The organic material was first introduced in the solar cell by Calvin in the 1960s [12]. The idea of a multi-

junction solar cell came in 1970, and the layer of different semiconductor material was used in a solar cell to absorb a broad spectrum. The real breakthrough in the field of photovoltaic devices came with the introduction of two different photosensitive semiconductors instead of one semiconductor material by Tang in 1986 [13]. The German and French scientists built a multi-junction solar cell and recorded 46% power conversion efficiency in 2014 [14]. The solar cell development using various types of material in the different periods is categorized into four generations of the solar cells, as illustrated in Figure 1.2.

The present day's solar market is dominated by the first two generations [15], [16]. The first generation includes eminent and medium-cost technologies (i.e., mono or polycrystalline Si and GaAs based solar cells), which results in moderate yields. The second-generation mainly comprises thin film (TF) technology-based solar cells that are cheaper to manufacture but have lower efficiency [16]. Copper Indium Gallium Selenide (CIGS) and CdTe/CdS based solar cells are examples of the second generation. Then, the third-generation solar cells are very efficient but expensive as they explore the usage of novel materials and the variability of designs [17]. They involve technologies based on newer compounds, stacked or tandem multilayers of III-V materials (inorganics based), Quantum Dots (QDs), Dyed Sensitized Solar Cells (DSSCs), etc.

Finally, the fourth generation is currently under investigation and is also recognized as "Inorganics-in-Organics". It mainly syndicates the flexibility or low cost of polymer TFs with the efficient and stable novel inorganic nanostructures (such as metal oxides and nanoparticles) along with organic-based nanomaterials (like graphene or its derivatives, carbon nanotubes) [18]. The recent development in solar cell manufacturing

includes solar cells made of several organic, inorganic, and organometallic halide perovskite materials. The exceptional improvement in the power conversion efficiency from 3.8% to 25.2% in the perovskite solar cell (PSC) has been observed in a very short span of time. Moreover, the cost to manufacture a perovskite solar cell is a fraction of the cost of other thin-film technology with almost equivalent performance. Although PSC has lower stability over time, it has several advantages, such as low-temperature solution processing and the ability to produce a flexible solar cell. All these advantages and the availability of a wide range of perovskite materials can be used to fabricate more exciting and appropriate solar cells.

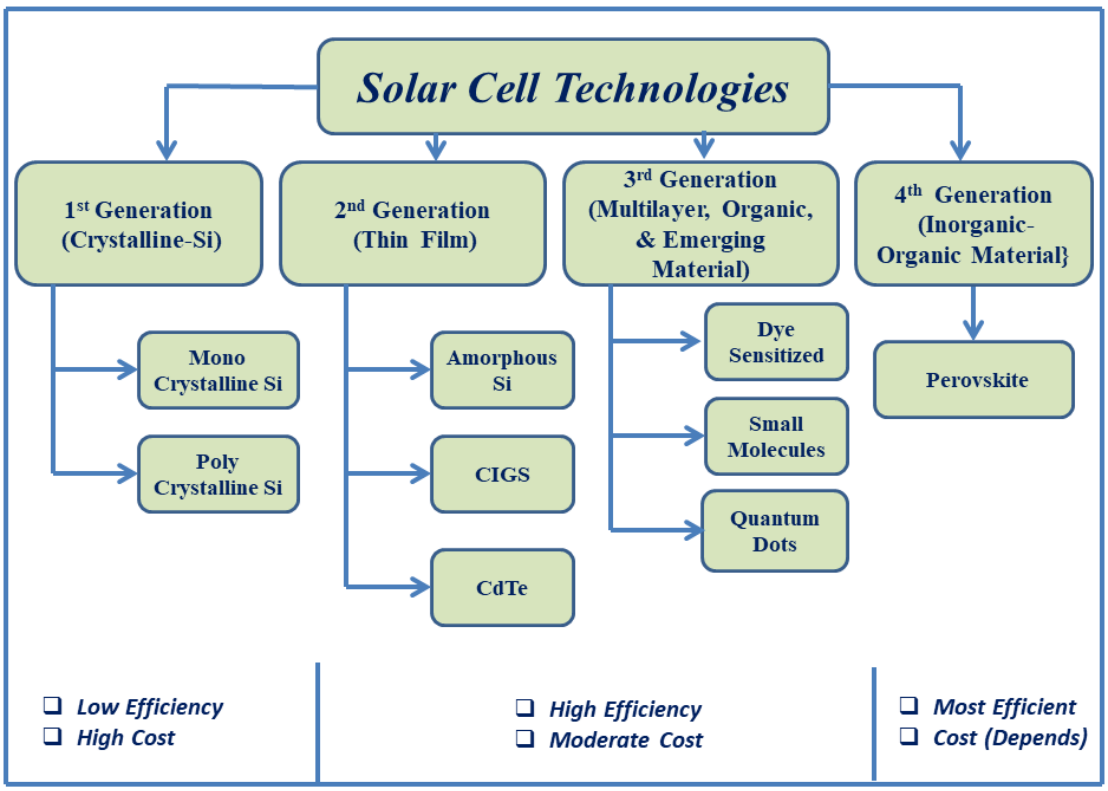

Figure 1.2: Different generations of solar cells.

1.2 Perovskite Solar Cell

Perovskite solar cell comes under the most recent generation of the solar cell. It has the inherent advantage of high efficiency, low cost, and easy fabrication process. The PSCs are made using perovskite structured material as photoactive. The efficiency of the PSC depends mainly on the perovskite material used. The achieved efficiency for perovskite solar cells is comparable to the Si and other materials-based solar cells' efficiency, as shown in Figure 1.3. The improvement in the PCE has been achieved by optimizing the thin-film processing technology and bandgap engineering of the perovskite film in the solar cells [19]. Efficiency has also been enhanced by choosing a suitable wide bandgap organic or inorganic material for electron transport layers (ETLs), hole transport layers (HTLs), and bandgap alignment in the device structure. Moreover, the defects such as pinholes and grain boundaries created during the fabrication process and the material properties such as extinction coefficient, carrier mobility, diffusion length, bandgap, etc., affect the PCE of the solar cells.

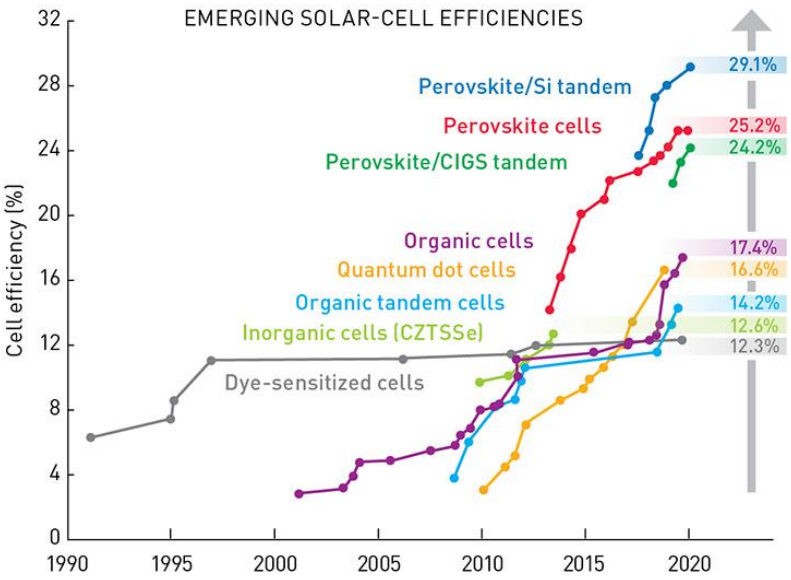

Figure 1.3: Comparative rapid growth in PCE for perovskite-based solar cells [20].

1.2.1 Perovskite Material

Perovskite material was first discovered by the Russian mineralogist Gustav Rose in 1839 in a piece of chlorite rich skarn. The mineral was $CaTiO_3$, named after the legendary Russian mineralogist Count Lev A. Perovskiy [21]. Later, the name perovskite was also referred for the three-element metal oxides such as $PbTiO_3$, $BiFeO_3$, $BaTiO_3$, etc., having a perovskite structure with the formula ABO_3. These metal oxides find use in several ferroelectric, dielectric, pyroelectric, and piezoelectric applications. Nowadays, the name perovskite does not only refer to metal oxides but also to halides, which have halide anions (F^-, Cl^-, Br^-, I^-) in place of oxide anions (ABX_3; A = cation, B = divalent metal cation, X = halogen anion). The halide perovskite was discovered by Well et al. in 1893 during their experiments on the synthesis of cesium-based lead halide compounds, $CsPbX_3$ (X = Cl, Br, I) [22]. The real breakthrough for the perovskite occurred in 1957, when C. K. Møller, a Danish researcher, reported that $CsPbCl_3$ has the perovskite structure [23].

The first three-dimensional organic-inorganic hybrid perovskite was discovered by replacing cesium in $CsPbX_3$ (X = Cl, Br or I) with methylammonium cations (MA = CH_3NH_3+) by Dieter Weber in 1978 [24]. The organic-inorganic hybrid perovskite ($CH_3NH_3PbI_3$) is most commonly used as photoactive material for making highly efficient photovoltaic and optoelectronic devices. The lead halide perovskite materials possess unique and much suitable semiconductor properties such as high absorbance coefficient, direct bandgap, large diffusion length, etc., which allow them to manifest into efficient photovoltaic cells and other optoelectronic applications such as light-emitting diodes (LEDs), photodetectors, X-ray detectors, and so on. Despite their eccentric electronic and optoelectronic properties, the two major issues are that stability

and toxicity of the perovskite materials have held up their commercial applications in the current scenario. In this thesis, 3D organic-inorganic lead halide perovskites have been analyzed for photovoltaic applications.

1.2.1.1 Crystal Structure

The crystal structure of hybrid perovskite compounds is similar to $CaTiO_3$ or in more general form ABX_3. Typically, the 'A' atoms are larger than the 'B' atoms. The 'A' and 'B' cations coordinate with 12 and 6 'X' anions, respectively, to form cuboctahedral and octahedral geometries, as shown in Figure 1.4.

Table 1.1: Comparison of optical properties of perovskite with other materials.

Material	Band Gap	$q.V_{OC}$ (eV)	Energy Loss (eV)
GaAs	1.43	1.12	0.31
Perovskite	1.55	1.19	0.36
Silicon	1.12	0.74	0.38
CIGS	1.15	0.76	0.39
CdTe	1.49	0.88	0.61
a-Si	1.6	0.9	0.7

The halide perovskites have semiconducting properties that are highly desirable for photovoltaic (PV) and other optoelectronic applications. The essential parameters of perovskite are compared with other common materials used for solar cell fabrication and listed in Table 1.1.

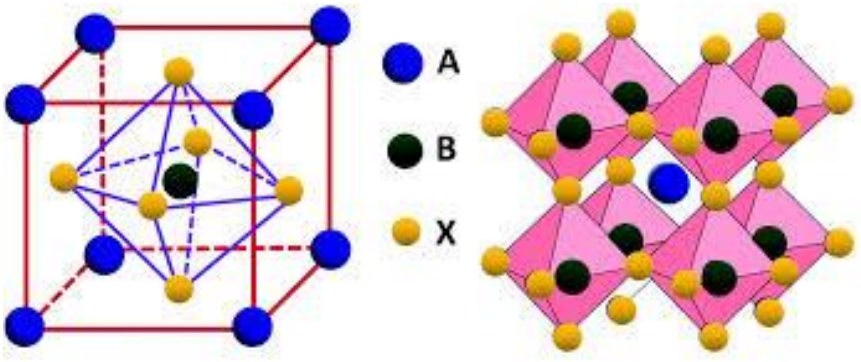

Figure 1.4: (a) Structure of ABX_3 perovskite (b) Cubic unit cell of $CH_3NH_3PbI_3$ [25].

1.2.1.2 Optoelectronic Properties

The ionic nature of organic-inorganic halide perovskite materials and their semiconducting properties, i.e., allow a free tuning of absorption edge wavelength (bandgap) and optical absorption by varying or combining halide ions (Cl, I, Br), thereby developing mixed-halide solid solutions. Methylammonium lead iodide ($MAPbI_3$) is a unique intrinsic semiconductor [26] showing superior mobility of both photogenerated holes and electrons. Figure 1.5 illustrates the band diagram for $MAPbI_3$, where the valence band (VB) incorporates nearly ~25% Pb $6s^2$ orbitals (lone pair) and 70% I 5p orbitals, while the conduction band (CB) contains a mixture of $6p^2$ orbitals of Pb and several other orbitals. In such a case, there exists strong coupling in VB orbitals between I 5p orbitals and Pb lone-pair $6s^2$ [27]. The structure of $MAPbI_3$ is highly symmetric, which results in the direct bandgap in this material. Moreover, Pb s orbital lone pair enables p-p electronic transitions from VB to CB. Therefore, the combination of these factors imparts extraordinarily high optical absorption coefficients to $MAPbI_3$ ($\sim 10^5$ cm^{-1}) [28]. The acclaimed defect tolerant properties of perovskite material are credited to its ionic characteristics, strong I p-Pb s anti-bonding coupling, and weak I p-Pb p coupling [27]. This property is replicated by the $MAPbI_3$ having large carrier

diffusion lengths. Moreover, as $MAPbI_3$ is an intrinsic semiconductor, it has ambipolar carrier mobility owing to its ionic crystal. On a final note, recombination between electrons and holes is suppressed in halide perovskites due to a charge-screening effect against Coulombic interaction, which is assisted by the high ionic density of the perovskite.

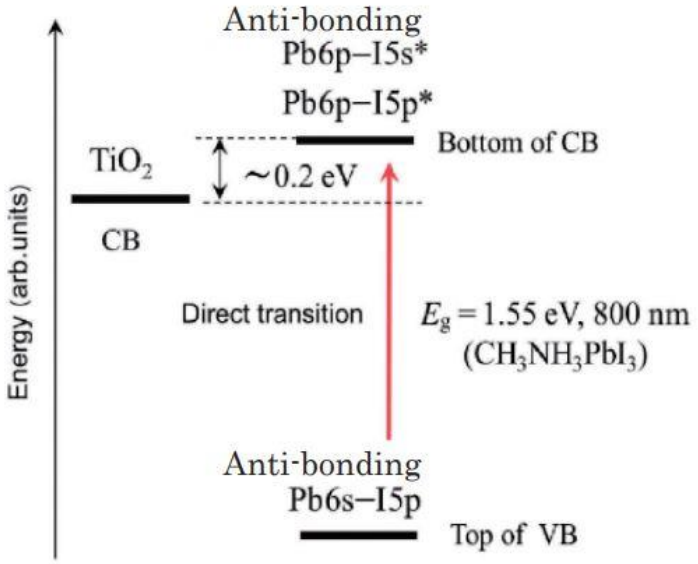

Figure 1.5: Band structure of $MAPbI_3$ [29].

The optical bandgap of the hybrid perovskite material can be tuned by the changing in "A" site cation and "B" site cation [30]. Perovskite quantum dots (QDs) offers tunability with size, which can be controlled using changing the concentration of the capping agents or surfactants (octyl amine and oleic acid) [31]. $CH_3NH_3PbI_3$ also has the ability to be used in photodetector because it shows the high gain of the photoinduced current, which exceeds 100%. Nowadays, perovskites have potential use for color image sensors in digital cameras. The perovskite-based color sensors and photodetectors take advantage of the low-cost and printable semiconductors and are expected to be commercialized soon. Perovskites are also used for the detection of X-

Rays in the medical diagnosis. It works well because lead-based perovskites have high absorption coefficients for X-ray radiation. Samsung's research group and Park et al. reported the detection of an actual X-Ray image by using a 2D patterned image sensor [32]. Organic lead halide perovskite-based optoelectronic semiconductor devices may also be used as radiation sensors for space explorations owing to their high defect tolerance nature.

1.2.2 Working Principle of Perovskite Solar Cells

The perovskite-based solar cells are commonly made in p-i-n structure, as shown in Figure 1.6. The organic-inorganic hybrid perovskites (i.e., $CH_3NH_3PbI_3$, $CH_3NH_3PbBr_3$, $CH_3NH_3PbI_3$, etc.) are used as intrinsic (i) layer and work as photoabsorber. The wide bandgap conducting polymers (i.e., spiro-OmeTAD, PTAA, etc.) and metal oxides (i.e., TiO_2, ZnO, etc.) are used for the p and n layer, respectively. The photovoltaic operation in the p-i-n structured perovskite solar cell is based on three basic concepts: (a) Generation of charge carrier in absorber (i) layers, (b) Separation of charge carrier by transport (p and n) layers, and (c) Collection of charge carrier at electrodes. When the solar cell is illuminated with sunlight having photon energy (hv) greater than the bandgap (Eg), the photon is absorbed by the absorber layer, and the charge carrier is generated. Due to the internal electric field, the electron-holes pair are separated by consecutive electron and hole transport layers. If these charge carriers are not separated, they will recombine shortly. Finally, the charge carrier is collected by the top and bottom electrodes of the solar cell and creates the photovoltage across the device. The polarity of the output voltage is the same as the "forward bias" direction of the device, but the photocurrent is opposite to the direction of the forward current through the

device under dark condition.

Solar light causes a current (I) to flow from the solar cell to the load. The magnitude of this current (I) is the algebraic sum (without sign) of generated current (I_{PH}), the current flowing in the non-linear junction (I_D), and the current passing through shunt resistance (I_{SH}). The equivalent electrical circuit of the solar cell has been shown in Figure 1.7. The I-V characteristics equation for the equivalent electrical circuit of the solar cell under illuminating condition is given as,

$$I = I_{PH} - I_S\left[exp\left(\frac{V + I \times R_S}{V_T}\right) - 1\right] - \frac{V + I \times R_S}{R_{SH}}$$

where I_{PH} is photogenerated current, I_S is reverse saturation current, and V_T is the thermal voltage.

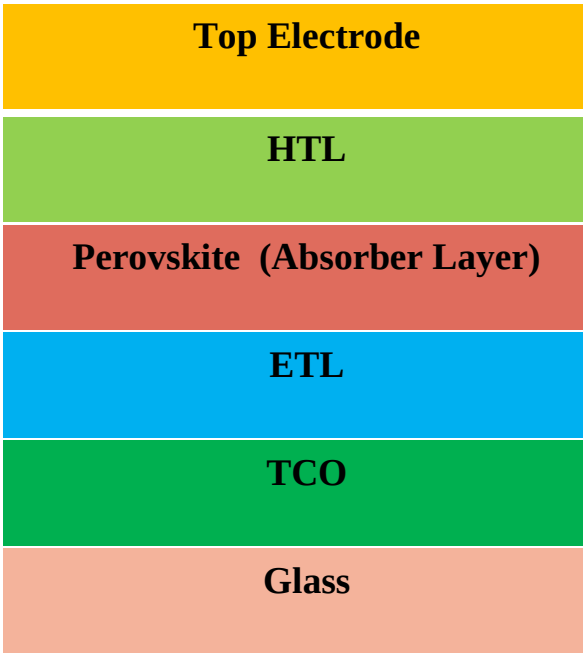

Figure 1.6: General structure of perovskite solar cell.

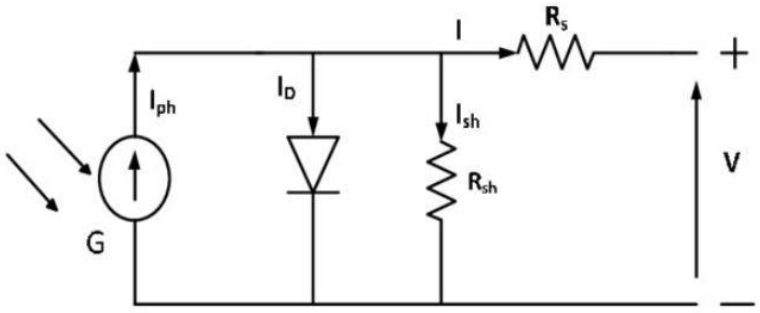

Figure 1.7: Electrical equivalent model of the perovskite solar cell [16].

It is evident from the I-V characteristic equation that solar cell parameters are greatly affected by series and shunt resistance. The impact of series resistance and shunt resistance on solar cell parameters are analyzed by the equivalent circuit shown in Figure 1.7. The series resistance R_S, represented in the equivalent circuit, can arise due to the contact resistance, resistance of semiconducting layers, and the contact resistance of electrodes. The shunt resistance, R_{SH}, can similarly be caused by various factors, such as surface leakage along the edge boundaries, crystal defects, or pinholes in the surface. The thickness of the different layers is also a factor that changes the resistance of the device and affects the performance of the solar cell. It can be observed that the zero value of R_S and the infinite value of R_{SH} gives the best performance (ideal case).

The performance of the solar cell is specified using four main solar cell parameters, namely open-circuit voltage (V_{OC}), short circuit current (J_{SC}), fill factor (FF), and power conversion efficiency (η). The electrical equivalent model, shown in Figure 1.7, and the current density-voltage (J-V) curve, shown in Figure 1.8, are used to analyze these characteristics of the solar cell. For all the values of J and V, the product of these two quantities gives the power density ($P=J\times V$), and the product has a maximum value (called Pmpp) at a particular current and voltage value (called Jmpp and Vmpp). The short circuit current density and open-circuit voltage are described as:

I (at V=0) = I_{SC} and

V (at I = 0) = V_{OC}

Or

$I_{SC} = I_m = I_\ell$ *and* $V_{OC} = V_m$ for forward-bias power quadrant

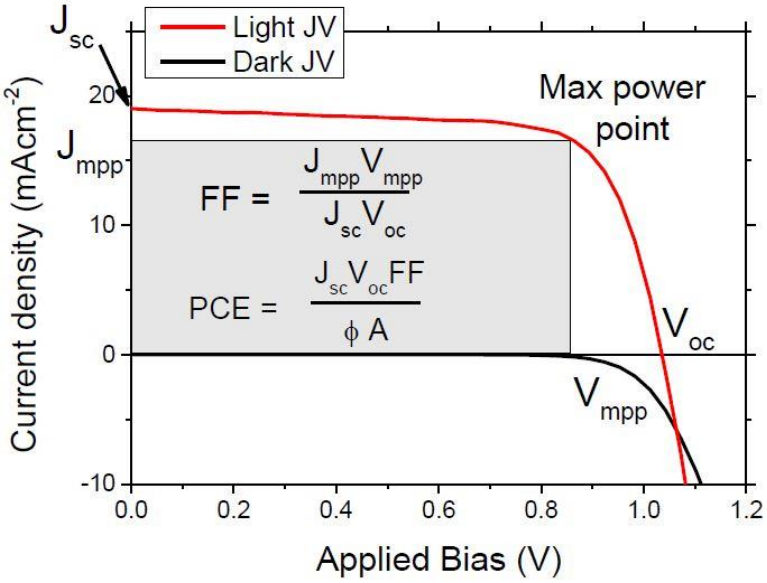

Figure 1.8: J-V curve for PSC device where the red curve is for under illumination and black is for dark. The area in the shade gives maximum achievable power.

On the other hand, the fill factor (FF) is evaluated by comparing the maximum power to the theoretical power (P_T). The fill factor also reflects the J-V curve's squareness, which represents the effects of resistive and recombination losses. The fill factor depends on open circuit voltage and short circuit current density, so there can also be a reduction in short circuit current below the value of the photocurrent due to the forward biasing across the junction as a result of the voltage drop across the series resistance (R_S). Finally, power conversion efficiency (η) is defined as the ratio of output energy of the solar cell (P_{MPP}) to the incident optical power density from the sun (P_{in}). PCE can also be written as,

$$\eta = \frac{Output}{Input} = \frac{I_m V_m}{\sum nh\upsilon} = \frac{V_{OC} J_{SC} FF}{P_{in}}$$

1.2.3 Numerical Modelling of Perovskite Solar Cells

A numerical simulation-based modeling approach is performed to develop a highly efficient solar cell, obtain optimum solar cell parameters, and understand the device physics. The fabrication cost can be minimized by optimizing device characteristics using technology computer-aided design (TCAD) simulation. Several TCAD simulation tools, such as SCAPS-1D, Lumerical, AMPS, SETFOS (Fluxim), etc., are available for the electrical and optical simulation of organic and hybrid perovskite solar cells [33]. Among these two popular tools, SCAPS-1D and SETFOS™ (Fluxim) are used in the present thesis work for the validation of the experimental results.

The numerical simulation model for the DSSC, silicon solar cell and other hybrid solar cells explains the behavior of the charge movement and the factor that affects the performance of the device. The performance of DSSC is based on the redox level in electrolytes, so the model includes a solvent that conducts ions and current. Similarly, the simulation models of the silicon-based photovoltaic device involve the doping that forms the p-n junction. The working principle of the perovskite solar cell is different from DSSC and silicon solar cells. The redox level and doping level is not required for the PSCs simulation model. Electrons and holes contribute to the current generated by photons energy in the PSC. So the numerical simulation plays a vital role in understanding carrier transportation mechanism and device performance.

The SCAPS-1D simulator can efficiently simulate the CIGS, CdTe, and crystalline solar cell (Crystalline Si and GaAs), which comprises up to 7 layers, whereas SETFOS can also be used for simulation of organic LED, solar cell as well as tandem solar cell structure with different layers. The simulation and modeling of hybrid perovskite solar cells are reported first time by Agrawal et al. [34] in 2015. The SETFOS simulation tool includes four different types of models, such as drift-diffusion, absorbance, advanced optics, and emission for a solar cell with a fitting and optimization algorithm. The Emission module deals with dipole emission, full-spectrum, color filter, and substrate optics, whereas the scattering module helps in improving the optical efficiency of the material. The charge generation, recombination, and transportation profile are managed by the absorption and drift-diffusion modules. The basic parameters required for electrical simulation are electron affinity (X), Bandgap (Eg), dielectric constants, the density of states of the conduction band and valence band (N_C and N_V), mobility of electrons and holes (μ_e and μ_h), the thermal velocity of electrons and holes, doping concentration of acceptor and donor (N_A and N_D), absorption coefficient, defect density (N_t) of different layers and also working temperature.

In these simulation tools, there is the flexibility to choose parameters either graded or different profiles. Optically we can separately define reflection, transmission, and other parameters. It also provides the option to vary the illumination spectra such as AM1.5G, AM0, AM1.5D, etc. SCAPS-1D provides generation- recombination status, energy band, quantum efficiency, and J-V characteristics, which is used for the calculation of open-circuit voltage (Voc), short circuit current (Jsc), power conversion efficiency (PCE), and fill-factor. The sweep function is also available in the tools,

which is very useful for optimizing the performance of the solar cell by varying the material parameters such as thickness, defect density, doping, etc., of the different layers.

The simulation tools solve Poisson's equation for the electric field, which depends upon charge flow and trap centers in the material. Poisson's equation for a semiconductor can be stated as [35]:

$$\frac{d^2\phi(x)}{dx^2} = \frac{e}{\epsilon_0 \epsilon_r}\left(\rho(x) - n(x) + N_D - N_A + \frac{\rho_d}{e}\right)$$

The current density due to electron or hole at any point in the device must be identical at all the points under the steady-state condition in dark condition. However, generation and recombination affect the current density under illumination. The continuity equation for electrons and holes can be inscribed as [35]:

$$\frac{dJ_n}{dx} = G - R$$

$$\frac{dJ_p}{dx} = G - R$$

Also, the total currents are calculated from drift and diffusion components as [35]:

$$J_n = D_n \frac{dn}{dx} + \mu_n n \frac{d\emptyset}{dx}$$

$$J_p = D_p \frac{dn}{dx} + \mu_p p \frac{d\emptyset}{dx}$$

Where J_n and J_p are current densities due to electron and hole, G is generation rate R is recombination rate, ϕ is electrostatic potential, e is electric charge, ε_o is vacuum permittivity, ε_r is relative permittivity, p and n are electron and hole concentration, N_A and N_D are charged impurities of donor and acceptor and ρ_d is defect charge density.

The recombination models commonly used are band-to-band recombination, SRH (Shockley-Read-Hall) recombination, and Auger recombination, as illustrate in Figure 1.9. Band to band (rediative recombination) and Auger recombination are unavoidable because these are intrinsic material properties. Band-to-band recombination is the process in which the electrons fall back from the conduction band to the valence band to recombine with holes. The expression for the band to band recombination is given as [35]:

$$R = \gamma(n.p - n_i^2)$$

Where γ is the recombination coefficient. The SRH (Shockley-Read-Hall) recombination takes place due to the impurities and defects in a material. These defects create trap states, which are essential for this recombination; hence it is also called trap-assisted recombination. The rate of this recombination can be expressed as:

$$R_{SRH} = \frac{p.n - n_i^2}{(n + n_i) + \tau n(p + n_i)}$$

Where τp and τn are electron and hole lifetime, n_i is intrinsic carrier concentration.

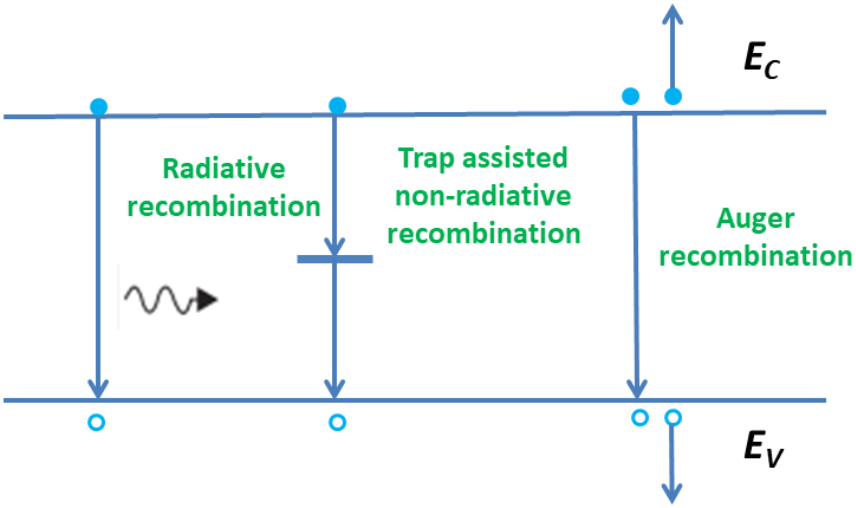

Figure 1.9: Band-to-band (radiative recombination), SRH, and Auger recombination.

SRH recombination occurs extensively when defects between crystal grains are present and cause increased trap states. Therefore, single-crystal materials have generally lesser SRH recombination due to extrinsic impurities and dangling bonds at the surface. In Auger recombination, the energy released by a band to band recombination of an electron-hole pair is given to another carrier. It can be expressed as [35]:

$$R = (C_n^A + C_p^A)(np - n_i^2)$$

Where C_n^A and C_p^A are constants.

1.3 Fabrication Process for Perovskite Solar Cells

The perovskite solar cell is a multilayered thin-film device. The different layers, namely electrodes (anode and cathode), photo absorber, hole transport layer, electron transport layer, and other interface layers, are composed of different materials in the

solar cell structure. Some key processing steps should be considered for high-performance solar cells. First of all, a suitable bandgap material (absorber material) is chosen to absorb the maximum solar light spectrum, the next one is selecting the wide bandgap electron and hole transport material to separate maximum charge carriers, and finally, the suitable work function material for electrodes are required to collect the maximum charge carriers. This section briefly discussed the various layers of perovskite solar cells.

1.3.1 Electrodes

The suitable top and bottom electrodes are used for better collection of charge carriers to get high-performance solar cells. Different physical vapor deposition (PVD) techniques such as sputtering, thermal, electron beam, etc., are commonly used to obtain a thin film of metals (Al, Ag, Cu, Au, Pd, Pt, etc.) and doped semiconductors (ITO, FTO, etc.) for the electrodes.

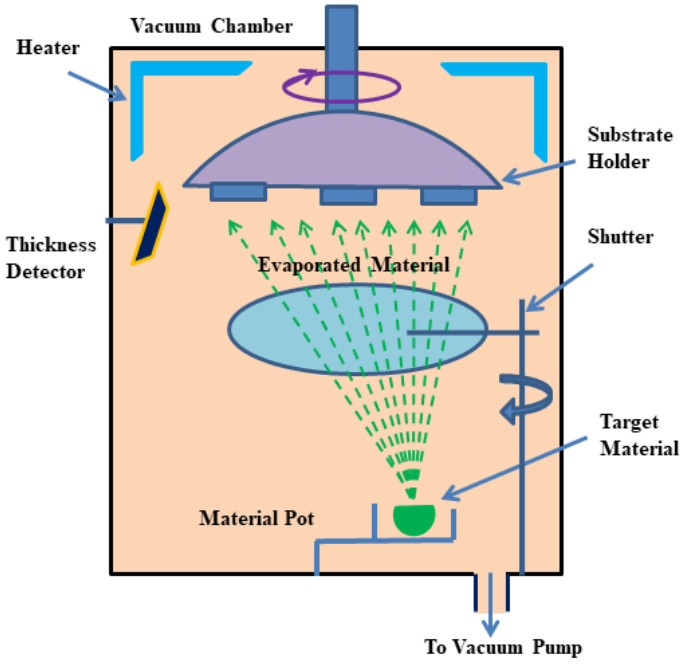

Figure 1.10: Block diagram of physical vapor deposition.

A block diagram of a typical PVD system is illustrated in Figure 1.10. The ITO/FTO is primarily deposited by the sputtering method and used as transparent conducting oxide electrodes at the bottom of the solar cell so that maximum light can pass through it. Noble metals, Au and Pd, with high work function (~4.8 to ~5.1 eV) are the most suitable top electrodes (avoiding fast oxidation and degradation) for perovskite solar cell is commonly deposited by thermal and electron beam evaporation. Thermal evaporation is also employed to deposition high purity Ag/Al film as a top electrode on both the solution-processed and thermally deposited metal oxide ETL.

1.3.2 Photoabsorber Layers

The photoabsorber layer is the most crucial layer, and perovskite material is used for this layer. The LUMO and HUMO level of hybrid perovskite material can be easily modified by using the composition of different halide anions (i.e., the composition of Cl, Br, and I in hybrid perovskite), and thus the absorbance coefficient changes. In the last few years, the power conversion efficiency of perovskite solar cells has been remarkably increased by gradual development in deposition techniques of perovskite thin film. The film coating controls the morphology and crystallinity of hybrid perovskite material that affects the absorbance coefficient of perovskite material and significant impact on short circuit current density. The stability of perovskite film also depends on the growth and crystallinity of perovskite material.

The high solar cell performances achieved in this short period are primarily due to the extensive efforts that have been invested over the years to develop and optimize these perovskite thin film deposition procedures [27]. These deposition methods include single step deposition [36], sequential deposition [37], vapor assisted deposition (via

single source and dual source) [38], screen printing, and anti-solvent methods [39]. Among these, sequential deposition and anti-solvent methods are two of the most widely used (methods) for the fabrication of solar cells. The PCE of hybrid PSC is achieved over 25.2% via sequential deposition technique [40]. In general, the spin coating deposition technique has enormous potential for the development of highly efficient perovskite solar cells for large scale production. Therefore, these achievements are very promising for the scale up of perovskite photovoltaics in the near future [27]. The three common deposition methods are discussed in following sub-sections:

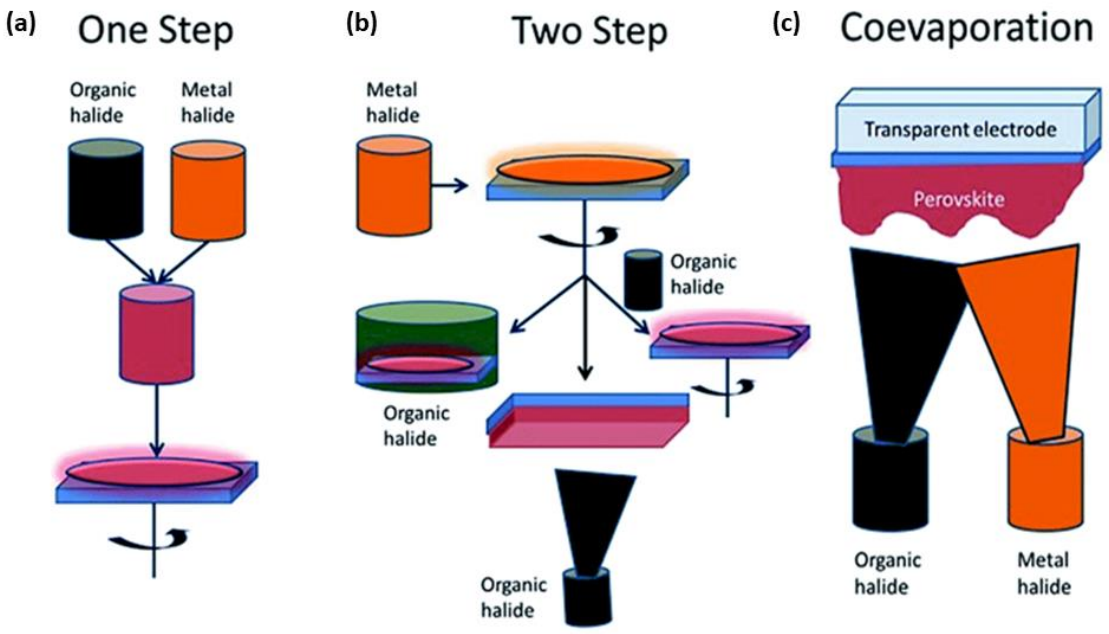

Figure 1.11: Deposition methods for the perovskite thin film: (a) One step deposition, (b) Two step deposition, and (c) Physical vapor deposition [41].

1.3.2.1 One Step Deposition via Spin Coating

The perovskite thin-film is initially deposited via spin coating in a single step on mesoporous metal oxide films using an equimolar ratio of PbX_2 and CH_3NH_3X in a common solvent [42]. Polar solvents, such as dimethylformamide (DMF),

dimethylsulfoxide (DMSO), g-butyrolactone(GBL), or N-methyl-2-pyrrolidone (NMP), are commonly used [43]. Spin coating is followed by heating the film at 70–150^{o}C to evaporate the high-boiling point solvent and in order to increase the grain size and crystallinity of hybrid perovskite ($MAPbX_3$) thin film [43]. The perovskite deposited substrate is converted from light yellow to dark brown after cooling at ambient temperature and confirmed the formation of perovskite film [42]. The problem with these deposition methods is that non-uniformity and uncontrolled grain size. Typically, it leads to uncontrolled precipitation of the perovskite with large morphological variations in photovoltaic performance in the resulting devices.

1.3.2.2 Two Step Deposition via Spin Coating

A sequential deposition method for perovskite thin layer is first employed by Liang et al. [28] to enhance the performance of PSC. For the preparation of organic-inorganic lead halide ($CH_3NH_3PbI_3$) thin film, the solution of organic compound (PbI_2) is infiltrated in the mesoporous layer of Al_2O_3 or TiO_2, and the film is dried by evaporating the solvent. In the 2nd step, the PbI_2 deposited substrate is dipped into the solution of organic compound (CH_3NH_3I). Conversion of perovskite thin-film occurs within the mesoporous when both the compound organic and inorganic comes into contact, permitting much better control over the perovskite morphology. The sequential deposition technique is further optimized for performance improvement of hybrid PSCs by Burschka et al. [37]. This significantly increased the reproducibility of device performance and achieved a PCE of approximately 15%. Further, with the development of technology, the anti-solvent technique has been employed for enhanced performance parameters of perovskite solar cells. Jeon et al. [44] have used an anti-solvent method

during deposition of perovskite thin film to fabricate highly efficient hybrid perovskite solar cells.

1.3.2.3 Vapor assisted deposition technique

Vapor assisted deposition process is a novel techniques for the deposition of high quality and uniform perovskite thin film. In this method, the first step includes the deposition of the inorganic compound via solution process followed by deposition of physical vapor of organic compound from a single source. This technique provides full surface coverage and moisture stability in a non-vacuum solution. The vapor assisted solution process is distinct from other traditional solution deposition techniques because it decelerates nucleation and permits robust reorganization of thin-film growth. Ping fan et al. reported a PCE of 10.90% for perovskite solar cells based on the single-source physical vapor deposition method [32]. The vapor deposition via dual-source process is used for well-defined grain structure, extremely uniform deposition, and full surface coverage of perovskite thin-film without post-heating treatment. But the simultaneous control of evaporation of both the organic and inorganic compound is very difficult to handle with dual-source evaporation methods.

1.3.3 Charge Transport Layers

Wide bandgap hole blocking and electron blocking materials are commonly used for ETL and HTL, respectively, in the PSCs. The structural and material engineering of the ETL and HTL plays an important role in the performance improvement of the PSCs. Efficiency can be enhanced by choosing a suitable wide bandgap material for ETL, HTL, and bandgap alignment in the device structure [45]. The primary function of the ETL and HTL layer is to extract the electron and hole from the absorber layer and

transport them to electrodes. The energy band alignment between HTL (ETL) and absorber layer plays an essential role for transportation of hole (electron) and blocking of the electron (hole) to minimize charge carrier recombination.

The structural, chemical, electrical, and optical properties of the charge transport layers (ETL/HTL) strongly depend on the deposition techniques and the environment under which the deposition of the materials is performed on the desired substrate. Various methods such as spin coating, thermal evaporation, electrochemical, hydrothermal, spray coating, screen printing, vapor deposition, chemical bath deposition, etc., are employed for the deposition of ETL and HTL of the solar cell. The comparison of various methods is listed in Table 1.2. The spin coating and screen printing (Blade coating, slot die coating), spray coating, hydrothermal, etc., are chemical solution-based, low-cost techniques. Metal oxide electron transport layers such as TiO_2 and ZnO are deposited by all techniques. However, the hydrothermal method is mostly used for the nanostructures (nanorods, nanowires, nanotubes, etc.) based thin film of TiO_2, ZnO, and other metal oxides at low cost and low temperature. The hydrothermal process provides a controlled size and shape of the nanostructures with highly crystallized and uniform.

Table 1.2: Comparison of different deposition techniques for charge transport layers.

Methods	**Advantages**	**Disadvantages**
Sputtering: Thin-film is deposited by ion bombardment of the source (target) by generated plasma on the desired substrate.	1. Large surface area deposition 2. Good reproducibility	1. It may be surface damage in the substrate used. 2. A high-cost vacuum chamber is required
E-beam evaporation: The electron beam is used to deposition thin-film by the transformation of atoms into the gaseous phase.	1. Good for liftoff 3. Highest purity 4. High precision of film thickness 5. Ease of operation 6. Excellent material utilization	1. Some CMOS processes sensitive to radiation and heat 2. Difficult for alloys 3. Poor step coverage and decomposition 4. A high-cost vacuum chamber is required
Chemical bath deposition (CBD): The thin film layer is deposited by dipping substrates in solutions with ions of interest (particularly metal ions).	1. Simple and low-cost experimental set up requires 2. Easy Control of the thickness of the film	1. Lack of reproducibility compare to other chemical deposition methods
Sol-Gel: This method is based on inorganic polymerization reactions in which colloidal solution is used for deposition of the thin film of metal oxide. It includes four steps: hydrolysis, polycondensation, drying, and thermal decomposition.	1. Excellent composition control 2. Can be used for large scale production. 3. Low cost and low-temperature technique	1. Film thickness control 2. Optimization for the particle size of the colloidal solution required 2. Surrounding environment affects the film 3. Porosity control is difficult 4. Multiple thin film layer may cause cracks
Chemical Vapor deposition (CVD): Deposition by chemical reaction of reactants at the substrate surface and energy for the reaction is provided by heat.	1. High purity 2. Relatively high deposition rates 3. High quality, high-performance thin film	1. High temperatures requirement 2. The precursors material should be volatile at room temperature
PECVD: The chemical vapor deposition the technique uses plasma to improve the yield and performance of the synthesis	1. Less temperature required 2. Good material properties of the deposited thin film.	1. In some cases, toxic precursors are needed 2. High-cost equipment 3. Plasma could damage the deposited thin films
Spray Pyrolysis: The traditional multisource CVD process can be converted to a single-source deposition process by spraying a solution onto a surface at an adequate temperature	1. Simple and low– cost method 2. Suitable for large scale deposition	1. Size of droplets of the initial solution is not the same which can lead to inhomogeneity in the material
Hydrothermal deposition: This is a simple deposition technique that requires a specific growth temperature under high pressure to synthesize single-crystalline material using an aqueous solution. This is commonly used for the deposition of TiO_2/ZnO nanorods.	1. Better control of size and shape of thin film 2. It is possible to obtain high crystallized nanostructures	1. Optimization is required for the process 2. Problems in reproducibility.

1.4 Characterization Techniques for Perovskite Solar Cells

The different types of characterization techniques are commonly used to analyze and verify different layers in the solar cell structure. The characterization includes surface, optical, and optoelectronic for the thin films and devices, as follows:

1.4.1 Surface Characterization

Some essential surface characterizations are performed to understand the basic properties of the synthesized perovskite and other associated materials in the solar cell structure. The brief discussion on these characterization tools are discussed in the following subsections:

1.4.1.1 Atomic Force Microscopy

Atomic force microscopy (AFM) is a surface imaging technique used to find the surface topography of the deposited film. It is a type of scanning probe microscopy (SPM) and is widely used for height, surface roughness, and magnetism measurements. The resolution of the AFM is in the order of a fraction of nanometer that is 1000 times higher than the optical diffraction limit. Surface imaging through AFM is taken place by measuring the force between the tip of the probe and the sample under process, as depicted in Figure 1.12 (a). Three modes of operations of the AFM are as follow:

Contact mode: The raster scanning of the sample with respect to the tip of the probe for a minimal area is taken place to obtain the image.

Non-contact mode: In this mode of operation, the probe oscillates at the resonance frequency, the sample under process is kept standstill, and the force between probe and sample is measured to get the exact image.

Tapping mode: It is somewhere between contact and non contact mode of operation and takes advantage of the above two. The sample is escaped from being damaged by incorporating intermittent contact.

1.4.1.2 Scanning Electron Microscopy

Scanning electron microscopy (SEM) is a powerful tool to get the morphological, topographical, and compositional information of the sample through a focused beam of electrons. High resolution (better than 1 nanometer) image is produced by raster scanning of the electron beam and combining the beam's position with the detected signal, as depicted in Figure 1.12 (b). The most common mode of operation of the SEM is the detection of the secondary electron emitted by the atoms excited by the electron beam. The topographical image of the sample is produced by detecting the number of secondary electrons emitted by atoms excited by the electron beam. Energy dispersive X-ray (EDX) attached with SEM is used to find the elemental composition of the sample. Data produced by EDX analysis shows spectra consist of unique peaks corresponding to the elemental composition of the material.

1.4.1.3 Transmission Electron Microscopy

Transmission Electron Microscopy (TEM) is a technique to study the topography, morphology, composition, and crystallography of the material. TEM utilizes high energy electrons and electromagnetic lenses for characterization, as depicted in Figure 1.12 (c). TEM generates high-resolution images with a maximum resolution near 0.5Å. The selected area electron diffraction (SAED) pattern is primarily used for crystallographic measurement utilizing the wave nature of electrons instead of particle

nature. A high energy (~100-400 keV) parallel beam of the electron is passed through the sample. The electron beam has a wavelength in the nanometer range compared to atom spacing in the prepared sample. Electrons are diffracted by atoms of the material, and the scattering angle defines the crystal structure of the sample.

1.4.1.4 X-Ray Diffraction

X-ray Diffraction (XRD) is a widely used tool to extract information about crystal structure, phase, texture, and other parameters such as average grain size, defects, etc., of the nanomaterial. Data produced by XRD analysis is based on the diffraction pattern, as depicted in Figure 12 (d). The X-Ray strikes on each set of lattice planes of the sample at a specific angle in the process of the extraction of the sample information.

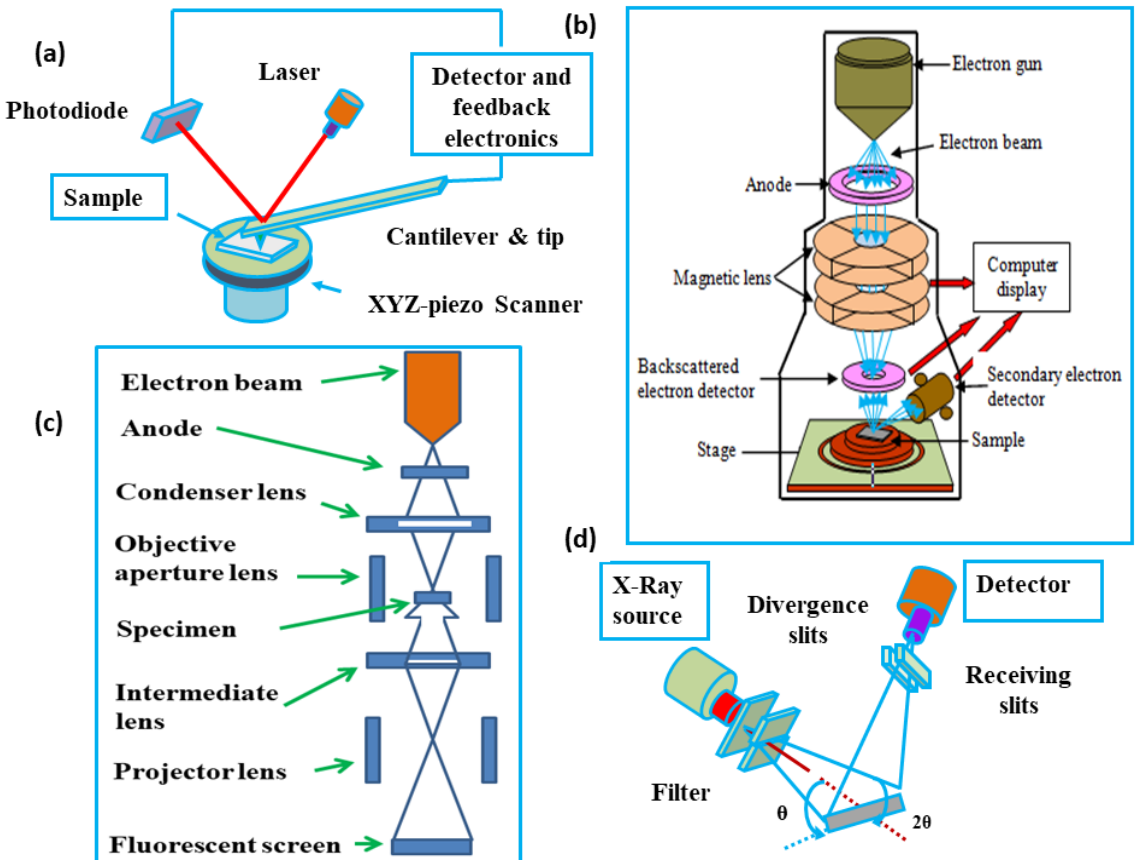

Figure 1.12: Meaurement setup for (a) AFM (b) HRSEM, (c) TEM, and (d) XRD.

1.4.2 Optical Characterizations

The optical characterization technique is a non-contact and non-destructive type analysis. It is commonly used to find the parameters such as absorbance, reflectance, transmittance, emission, film thickness, crystal structure, optical constant, etc., of the sample under investigation.

1.4.2.1 Absorbance

The absorbance technique is an extensively used technique for the evaluation of various parameters, namely absorbance, reflectance, transmittance, film thickness, crystal structure, optical constant, etc. The absorbance is also measured in reflectance and transmittance mode. It is also used to study the spectral composition of the light reflected from the surface with respect to the angularly dependent intensity and the composition of the light initiated from the light source. This study provides the film thickness as well as refractive index, coating homogeneity, and the other optical constant. Absorbance is primarily measured using the UV-Vis spectroscopy technique, as depicted in Figure 1.13 (a). In this technique, UV/visible light is passed through the sample, and the difference in intensity after transmission gives information about the optical characteristics of the sample.

1.4.2.2 Photoluminescence

The photoluminescence technique is a powerful non-contact and non-destructive type technique widely used to extract information about the electronic structure of the semiconducting materials. Under light illumination, photoexcitation occurs by absorbing the light and imparting the excess energy into the material. This excess energy can be dissipated in the form of light emission called photoluminescence, as

depicted in Figure 1.13 (b). Data generated by this analysis provides excitation and emission peaks corresponding to the materials, and based on these peaks electronic structure of the corresponding material is extracted.

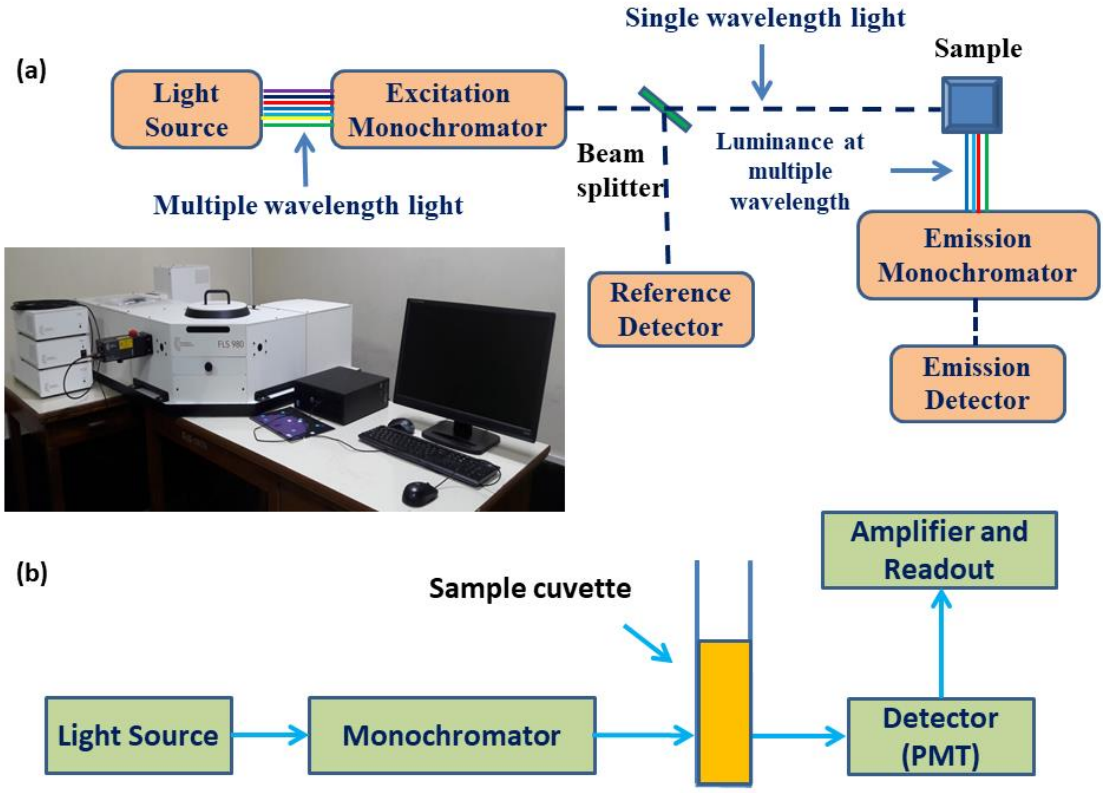

Figure 1.13: Measurement setup for (a) Photoluminescence spectrometer and (b) UV-Vis absorption spectroscopy.

1.4.3 Optoelectronic Characterizations

Electrical characterization of semiconducting materials or devices plays an essential role in examining its suitability for the integrated circuit used in different kinds of electronic devices such as mobile phones, computers, digital cameras, etc. The electrical characterization of electronic devices is called electronic characterization, and the measurement of change in electronic characteristics under optical illumination is called

optoelectronic characterization. The complete experimental setup for the measurement of various electrical and optoelectronic characteristics is depicted in Figure 1.14.

Current (I)-voltage (V) characteristic of any device shows how the current flowing through the device is being changed with respect to the voltage applied on terminals. An I-V characteristic is very crucial to evaluate various device parameters such as ideality factor, barrier height, etc. Capacitance (C)-voltage (V) characterization of any device represents the relationship between junction capacitance and the voltage applied across the terminal of the device. C-V characteristics are junction dependent and are used in the calculation of barrier height, carrier concentration, and depletion width. Impedance spectroscopy is used to study the resistance or capacitance properties of the device by applying the AC sinusoidal excitation signal. On the other hand, the I-V characteristics under dark and solar light illumination are used for the evaluation of various solar cell parameters.

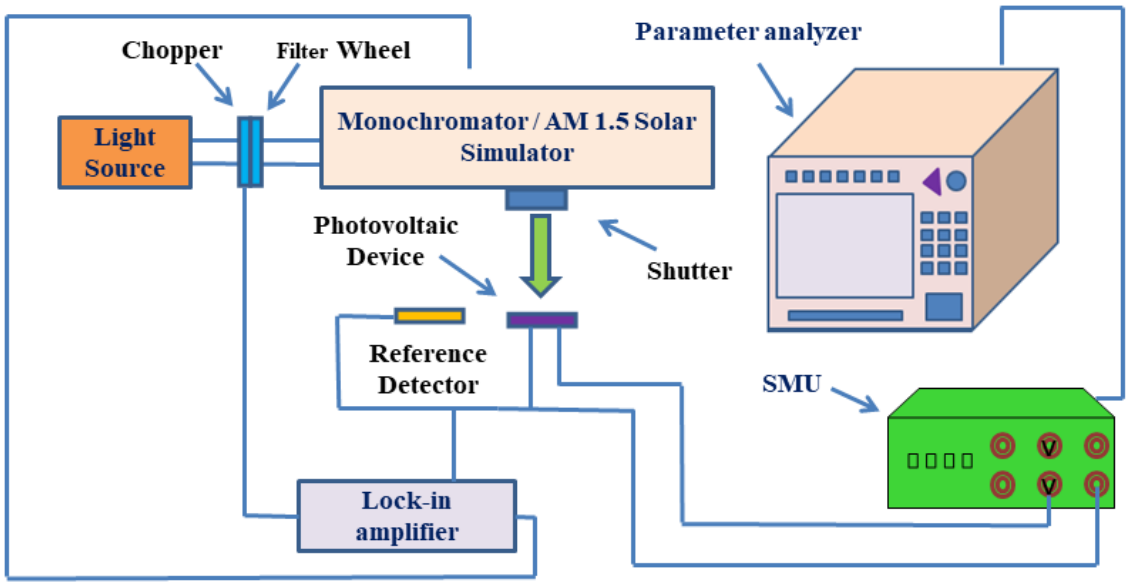

Figure 1.14: Optoelectronic characterization setup for perovskite solar cells.

1.5 Literature Review

This section aims to summarize the gradual development of perovskite solar cells and the detailed discussion on hybrid perovskite-based solar cells. First of all, the perovskite solar cell with different hole transport materials and some additives have been reviewed. Later, some crucial works on TiO_2 and ZnO nanorods based hybrid perovskite solar cells have been reviewed.

1.5.1 Review of Perovskite Based Solar Cells

The inorganic-organic hybrid perovskite is the emerging photosensitive material for photovoltaic applications due to its high absorbance coefficient and suitable bandgap [46]. The journey of perovskite solar cells began in 2006 with a power conversion efficiency (PCE) of 2.2% by Miyasaka et al. [47]. They have also reported the PCE of 3.1% and 3.8% by using $CH_3NH_3PbBr_3$ and $CH_3NH_3PbI_3$ sensitizers, respectively, in the dye-sensitized solar cell (DSSC) [48]. Considerable efforts have been made in the last few years to improve the PCE of the hybrid perovskite solar cells (PSCs) to near 25% [49]-[53], as depicted in Figure 1.15.

Perovskite sensitizer used with liquid electrolyte faced serious stability issues in the solar cell structure. In 2008, Miyaska et al. have employed a solid-state hole transport layer in PSC and fabricate carbo/conductive polymer composite based first solid-state PSC with PCE of 1% [54]. Later, Gratzel et al. reported Sb_2S_3 and poly(3-hexylthiophene) (P3HT) based solid-state perovskite photovoltaic device with 5.13% PCE [55]. Park et al. fabricated the first perovskite solar cell based on perovskite quantum dot (an equimolar mixture of the organic and inorganic compound in g-

butyrolactone solvent) and achieved PCE of 6.5% in 2011 [56]. Later, Park et al. made a full solid-state device by employing nanoparticles (NPs) of $CH_3NH_3PbI_3$ as a light sensitizer on mesoporous ETL and recorded the PCE of 9.7% in 2012 [57]. Snaith et al. fabricated solar cells by incorporating a new deposition technique (dual-source vapor deposition) for perovskite thin film and get an excellent PCE of over 15% in 2013 [58]. In 2014, Juan et al. investigated the impedance spectroscopy measurement for $CH_3NH_3PbI_{3-X}Cl_X$ solar cell and studied the physical parameters of carrier transport and recombination in compositions based perovskite thin film [59].

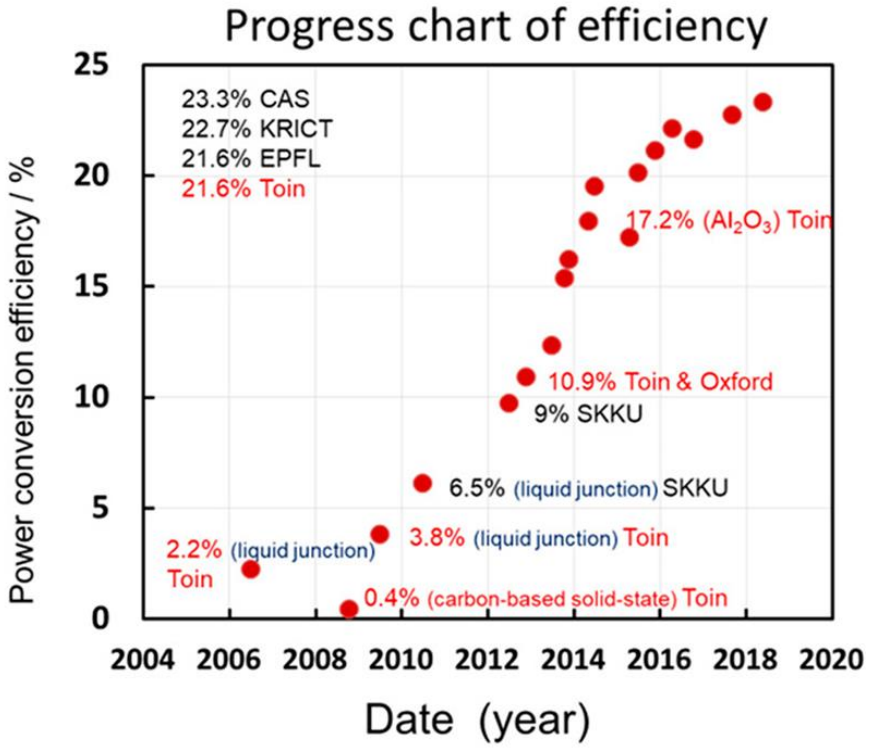

Figure 1.15: Progress in the power conversion efficiency of PSCs from 2006 to 2018 [60]

Further, Luo et al. [61] reported first-time perovskite nanowire-based hybrid solar cell and recorded 14.71 % PCE in 2015. Madhavan et al. [62] reported more than 20% PCE in 2D/3D perovskite-based PSC using CuSCN as a hole transport layer. They have also reported a photovoltaic device with photo-electrochemical systems that employ mesoscopic forms of semiconducting oxides as light absorbers. In 2015, Niu et

al. [63] investigated the chemical stability of perovskite material in different environmental conditions such as oxygen, moisture, UV-light, etc. The charge carrier transport behavior of quantum dots in perovskite material has been explained by Ning et al. [64], whereas the optical and electrical properties of perovskite material for photovoltaic and optoelectronic applications have been reported by Jung and Park [65] in 2015**.** Yang et al. [66] have investigated different electron transport layer-based perovskite solar cells in 2017. The performance of organic HTL and ETL based hybrid PSCs with a different annealing temperature for the perovskite layer have been studied by Jhong et al. in 2017 [67]. Hayase has reported a compositional mix of PbI_2 and SnI_2 based hybrid and toxic-free hybrid perovskite solar cell [68].

Furthermore, the performance of $CH_3NH_3SnI_3$-based solar cells with several types of HTM layers such as CuSCN, Cu_2O, and spiro-OMeTAD are optimized using the TCAD simulation [69]. The ZNRs are employed for ETL in all the PSC structures and achieved remarkable PCE of 18.34%, 20.23%, and 20.21% for CuSCN, Cu_2O, and spiro-OMeTAD based HTL. Li et al. [70] have grown ZNRs on the aluminum-doped ZnO seed layer and fabricated PSCs with the following structure: ITO/AZO seed-layer/ZnO-NRs/perovskite/spiro-MeOTAD/Au. They analyzed the surface preheating effect on parameter performance of ZNRs based PSCs and achieved optimum J_{sc} of 21.43 mA/cm^2, V_{oc} of 0.84 V, FF of 57.42%, and PCE of 10.34% with reduced pinholes in perovskite layer due to substrate preheating. P.S.Chandrasekhar et al. [71] demonstrated the performance of nitrogen-doped graphene/ZnO nanorod nanocomposites based PSC with improved device parameters photocurrent of 21.98 mA/cm^2 and PCE of 16.82% compare to without graphene-based PSCs.

1.5.2 Review of TiO_2 nanorods Based Perovskite Solar Cells

Various types of organic and inorganic materials such as PCBM, C_{60}, TiO_2, ZnO, SnO_2, and Al_2O_3 have been reported as ETL in the PSCs [72], [73]. Among them, TiO_2 is the most promising material for the ETL due to its large bandgap, high stability, and desired band bending with perovskite material [74]. The TiO_2 based ETL improves the stability of the PSCs and hence is mostly preferred over other metal oxides [73]. Different TiO_2 nanostructures such as nanotube, nanosheets, nanoparticles, nanorods, and nanowires have been used as ETL in highly efficient PSCs [75]-[78]. However, TiO_2 nanorod is preferred over other nanostructures in the PSCs due to its better charge transportation and robustness with perovskite materials [74].

Alberti et al. and Lozhkina et al. [79], [80] have developed thin solid-state hybrid solar cells composed of mesoscopic TiO_2, based solar cells using solution-printable processes. They have also developed other perovskite cell structures toward the realization of full printable technology of high-performance hybrid solar cells. The perovskite layer in PSC structure FTO/TiO2/Perovskite/SpiroOMeTAD/Au was fabricated via blade coating, and ETM/HTM material was deposited using thermal evaporation technique with an active solar cell area of 100 cm^2 by Razza et al. [77] and achieved 4.3 % PCE. Recently, Wan et al. [81] have improved the efficiency of CdS-sensitized TiO_2 solar cells by hydrothermal etching treatments of TiO_2 nanorods (TNRs). Priyadarshi et al. [82] introduced another deposition technique, drop cast for perovskite material for large area (70 cm^2) fabrication of PSCs structure of FTO/TiO2/ZrO2/Carbon/Perovskite and recorded 10.74% PCE. The PSC with 11.32% PCE based on an active area of 1.47 cm^2 was fabricated by Gao [83] using 50 nm

compact layer of TiO_2, spiro-OmeTAD based HTM layer by spin coating, and 300 nm thin perovskite layer via knife coating method.

1.5.3 Review of ZnO Nanorod Based Perovskite Solar Cell

The ZnO nanomaterials are among the most promising wide bandgap material for solar cell applications, LED, and photodetectors. ZnO is a widely used electron transport material due to its high mobility, easy synthesis, abundant availability, and high stability [84], [85]. In general, ZnO nanostructure is preferred in the ETL over its bulk counterpart due to the larger surface-to-volume ratio. The surface to volume ratio plays a vital role in photocatalytic activity [86]. Although 0D material (colloidal quantum dot) has a large surface to volume ratio, its use in perovskite solar cell structure is very less due to poor charge transportation. One dimensional material (ZnO nanorods) offers increased photocatalytic efficiency compared to bulk ZnO. Compared to other nanostructures, ZnO nanorods have fast electron transportation, a large conduction band, and high electron density. Son et al. [86] have reported the maximum PCE of 14.35% using (NH4)2TiF6 treated ZnO NRs based ETL in the PSC structure. Xu et al. [87] have obtained the PCE of 9.15% using ZnO NR (ZNR) arrays synthesized by modified solvothermal method.

Liu et al. have reported PCE of 15.4%% using ZnO ETL and vapor deposited hybrid perovskite material [58]. From the last two decades, there was some modification in the quality of single-crystalline ZNRs to improve the performance of optoelectronic and photovoltaic devices [88], [89]. Several techniques such as seed layer via spin coating, sputtering, chemical bath deposition (CBD), electrostatic spraying, atomic layer deposition (ALD) have been used for uniform growth of ZNRs

for minimizing the defects and traps [87], [90]–[92]. The bandgap of ZnO nanomaterials can be tuned by doping with some metal dopants like Al, Mg, and P. [88], [93], [94]. Shirazi et al. have also reported the ZNRs based HTL free hybrid PSC and achieved efficiency improvement by increasing the conductivity of ZNRs by Al doping [93]. Jeon et al. found the uniform and defect-free layer of perovskite when the toluene has been used as anti-solvent during spin coating deposition of perovskite thin film. The better phase formation and crystallinity of PbI2 with MAI (methylammonium iodide) are achieved when DMSO has been used as a solvent for PbI_2 precursor instead of DMF [44].

Peng et al. [95] minimized the decomposition of the hybrid perovskite layer by insertion of the SnO_2 layer on ZnO nanorods. The core-shell SnO2-ZnO nanostructures have been used to increase the oxygen vacancies at the ZnO-hybrid perovskite interface [95] for stabilization of perovskite later. The power conversion efficiency of hybrid PSC is significantly improved from 6.92% to 12.17%, and hysteresis is eliminated from the J-V curve by taking the core-shell nanostructure of the SnO_2-ZnO layer.

Zhang et al. [96] used a relatively fast and low temperature processed electrochemical method for deposition of ZnO layer and demonstrated low J-V curve hysteresis with PCE of 11% in the fabricated ZnO nanostructures based PSCs on ITO coated flexible substrate. The charge carrier mobility and charge recombination mechanism have also been investigated by Zhang et al. [97] for ZnO thin film deposited via electrospraying technique-based PSCs. They have also reported the performance of ZnO nanostructured based PSCs for perovskite thin film deposition via one-step and two-step deposition methods.

Later, several ZnO nanostructures deposited via different techniques such as pulsed laser deposition [98], electrophoretic deposition [99], PECVD [100], magnetic sputtering [101] have been explored for the fabrication of different types of PSCs structures, including planner [102], inverted planner [103], and mesoporous [97]. Kumar et al. [104] fabricated the perovskite/Spiro-OMeTAD/Au based PSCs with four different planner structure for ETL, namely FTO/ZnO(CL), FTO/ZnO(CL)/ZNRs, PET/ITO/ZnO(CL), and PET/ITO/ZnO(CL)/ZNRs. They have synthesized ZNRs using chemical bath deposition technique on FTO/ITO substrate with and without ZnO seed layer and recorded PCE of 8.90% for FTO substrates and 2.62% for flexible PET/ITO substrate-based PSCs.

1.5.4 Major Observation from the Literature Survey

The milestones achieved in the area of perovskite solar cells during their development are interesting to note [60]. It is observed that the period of 2013-2015 was focused primarily on the development of high-efficiency cells by using appropriate material selection and deployment of methods for high-quality perovskite film formation. This period also addressed issues regarding hysteresis and interfacial engineering. In 2016-2017, compositional engineering is applied widely, which resulted in improvement in both structural stability and efficiency. Extensive efforts are made to develop lead-free perovskites too. Now, after developing and optimizing methods of synthesis, the attention of researchers is on making the perovskite solar cell more stable for long-term use by addressing issues regarding light, moisture, oxygen, and thermal instability. Currently, attempts are made to scale up the production of solar cells for meeting industrial requirements, and the methods such as mechanochemical synthesis are

gaining popularity due to their solvent-free nature. Also, extensive research is being carried out in the area of all-inorganic halide based perovskites solar cells.

1.6 Issues and Challenges in Perovskite Solar Cells

The commercialization of hybrid PSC is still challenging because of toxicity issues (during fabrication, deployment, and disposal), long term chemical and phase stability, and cost-effectiveness. The perovskite material pertains to its stability and degradation due to moisture, oxygen, UV radiation, and temperature. The three major areas of thrust in perovskite research are: improving the material stability like phase stability, thermal stability, and replacement of the toxic heavy metal (Pb^{+2}). One possible modification has come through the substitution of cations, metal ions, and halogen to solve these challenges. Tin (Sn) is a candidate for the replacement of lead (Pb^{2+}) cation and can help in bandgap tuning of the perovskite material.

Compositional engineering is the leading interest in perovskite research for optimizing structure and usability governing factors. The hybrid perovskite decomposed in methylammonium, hydrogen iodide, and lead iodide in the presence of water. The prominent approach is the substitution of a methyl group with a bulky organic cation, leading to a 2D perovskite structure. The 2D layered and 3D bulk perovskite material can then be used to alternatively coat layers to prevent moisture impingement due to the hydrophobic nature of the alkyl group and avoid further degradation; however, with its own challenges such as disorientation, grain size improvement. Though, to enhance air stability, some butyl halide groups could be used. The compositional change by n-butyl ammonium iodide in the methyl group can yield towards low dimensionality. So, Goldschmidt tolerance factor will change accordingly based on the composition of

methyl and butyl group. A suitable tolerance factor will make a more stable perovskite material against moisture and oxygen.

1.7 Motivation and Problem Definition

It is discussed that the perovskite solar cells have some inherent challenges for commercialization. The identified challenges and their possible solutions are listed as follows:

- The 3rd generation of solar cells (organic solar cells) has low efficiency.
  - ✓ The absorbance coefficient of perovskite material is relatively more so efficiency can be improved by incorporating perovskite material.
- The low energy photons of solar spectrum (having energy less than the bandgap of active material) incident on photovoltaic device can't be converted into electricity and lost while the excess energy of high energy photon (having energy greater than the bandgap of active material) have been lost in heat form.
  - ✓ This can be easily overcome by changing the "A" cation of the perovskite material, and the suitable bandgap material (quasi-2D/3D perovskite) can be employed in PSCs for wide bandgap absorption.
- The efficiency of planar PSCs is less compare to mesoscopic PSCs.
  - ✓ The efficiency can be enhanced using TiO_2 and ZnO nanostructure in PSCs. The mesoporous layer (nanorods, nanowires, nanotubes, etc.) permits the perovskite photo absorber to penetrate mesoporous framework material, enhancing the absorption due to the high surface volume ratio of the perovskite material. So the incorporation of mesoporous material into PSCs improves the efficiency of PSCs.
- The planar perovskite solar cell has less stability

- ✓ By the incorporation of TiO_2 and ZnO NRs in PSCs, the stability can be improved. The monohydrate phase forms rapidly when the hybrid perovskite layer is deposited on a compact layer, but the decomposition rate of hybrid perovskite material is reduced when mesoporous scaffolds are employed.

Therefore, in this thesis, we focussed on optimizing the mesoporous n-type electron transport layer to improve the efficiency and stability of the perovskite solar cell.

1.8 Scope of the Thesis

The present thesis deals with the fabrication, characterization, and TCAD simulation of some $CH_3NH_3PbI_3$ hybrid perovskite-based PSCs using TiO_2 nanorods (TNRs)/ ZnO nanorods (ZNRs) as the ETL and Spiro-OMeTAD/PTAA as the HTL in the device. All the PSCs considered in the present thesis are of conventional n-i-p mesoporous device structure where the n-region represents the ZNRs/TNRs based ETL, i-region includes $CH_3NH_3PbI_3$ hybrid perovskite-based active layer, and the p-region represents the Spiro-OMeTAD or PTAA based HTL in the PSCs. The thesis consists of SIX chapters, including the present chapter. The outline of the remaining FIVE chapters is briefly described as follows:

Chapter 2 reports the fabrication, simulation, and characterization of FTO/TiO_2 Nanorods/$CH_3NH_3PbI_3$ (Hybrid-Perovskite)/PTAA/Pd structure-based perovskite solar cells (PSCs) where the FTO (fluorine-doped tin oxide) is the substrate, TiO_2 nanorods (NRs) layer acts as the electron transport layer (ETL), hybrid perovskite ($CH_3NH_3PbI_3$) is the active layer, PTAA is the hole transport layer (HTL), and Pd film acts as the contact electrode in the device. The TNRs are grown by the hydrothermal process followed by $TiCl_4$ treatment for enhancing the performance of the device. The

perovskite thin-film active layer and PTAA based HTL are deposited using the spin-coating technique. The effect of the ETL thickness on the performance parameters of the PSCs has been investigated and compared with the simulation data. The fabrication and characterization have been performed in open atmospheric conditions. The measured electrical and optical characteristics for three devices with three different ETL thicknesses were compared with the TCAD simulation results for comparing performance parameters of the proposed structure under real operating conditions and theoretically ideal conditions.

Chapter 3 investigates the effects of solvothermal etching and $TiCl_4$ treatment of the TiO_2 NRs based ETL on the performance of the FTO/TiO_2 NRs/$CH_3NH_3PbI_3$ /Spiro-OMeTAD/Pd PSCs. This study is carried out to basically show that not only the thickness of the ETL but also its surface morphology plays an important role in the performance optimization of the proposed PSC. Three different devices have been studied: The first device contains hydrothermally grown TNRs based ETL, the second device uses a $TiCl_4$ treated TNRs based ETL, and the third device uses solvothermally etched and $TiCl_4$ treated TNRs ETL, maintaining remaining parts of the device same as used in Chapter-2. The growth of other layers in the device is the same as considered in Chapter-2. Finally, the electrical and optical parameters are compared for all three PSC devices mentioned above.

Chapter 4 deals with the investigation of the effect of ZnO NRs ETL (grown on four different types of ZnO seed layers by hydrothermal method) on the performance of FTO/ZnO NRs/$CH_3NH_3PbI_3$/PTAA/Au based PSC structures. Four different types of seed layers of drop-casted ZnO film, spin-coated colloidal ZnO nanoparticles (NPs)

film, spin-coated colloidal ZnO quantum dots (QDs) film, and solvothermally grown ZnO NRs film were deposited on four FTO substrates. Then the seed layer coated FTO substrates were processed for growing ZnO NRs (of four different morphologies on four different seed layers) by the hydrothermal method. The $CH_3NH_3PbI_3$ perovskite active layer, PTAA based HTL, Au were successfully deposited for fabricating four different PSC devices under study. The surface morphologies of the four different types of ZnO NRs ETLs were studied by XRD and SEM analyses. The electrical and optical characteristics of the four PSCs with four different morphologies of ZnO NRs based ETLs have been studied in detail. The PSCs with ZnO NRs ETL grown on the ZnO QDs based seed layer showed better electrical and optical characteristics over the other devices.

Chapter 5 investigates the effects of doped and undoped Spiro-OMeTAD based HTL on the performance of FTO/ZnO NRs/$CH_3NH_3PbI_3$/Spiro-OMeTAD/Pd PSCs. The two types of hybrid-PSCs with doped and undoped HTLs were fabricated and characterized. Measured results were compared with the TCAD simulation data to validate the results measured under open atmospheric conditions.

Finally, **Chapter-6** summarizes the major observations and findings of the present thesis. Some future scopes of research related to this thesis have been outlined at the end of this chapter.